Spectrochimica Acta Part A: Molecular and Biomolecular Spectroscopy 187 (2017) 82–86

Contents lists available at ScienceDirect

Spectrochimica Acta Part A: Molecular and Biomolecular Spectroscopy

journal homepage: www.elsevier.com/locate/saa

An IR investigation of solid amorphous ethanol — Spectra, properties, and phase changes

Reggie L. Hudson

Astrochemistry Laboratory, NASA Goddard Space Flight Center, Greenbelt, MD 20771, USA

ARTICLE INFO

Article history:
Received 28 March 2017
Received in revised form 19 June 2017
Accepted 21 June 2017
Available online 21 June 2017

Keywords:
IR spectroscopy
Band strengths
Astrochemistry
Amorphous solids
Ices

ABSTRACT

Mid- and far-infrared spectra of condensed ethanol (CH_3CH_2OH) at 10–160 K are presented, with a special focus on amorphous ethanol, the form of greatest astrochemical interest, and with special attention given to changes at 155–160 K. Infrared spectra of amorphous and crystalline forms are shown. The refractive index at 670 nm of amorphous ethanol at 16 K is reported, along with three IR band strengths and a density. A comparison is made to recent work on the isoelectronic compound ethanethiol (CH_3CH_2SH), and several astrochemical applications are suggested for future study.

Published by Elsevier B.V.

1. Introduction

Some years ago our research group was engaged in the measurement of far-infrared spectra for upcoming NASA and ESA space missions involving infrared instrumentation. Most of our far-IR work was published at the time [1], and has since been used by astronomers and terahertz spectroscopists [2], but a new paper in this journal recently reminded us of some of our unpublished results. The focus of most of our research is infrared spectra of small-molecule amorphous and crystalline solids at 8–250 K, with an emphasis on amorphous ices below 100 K. Their IR spectra are used to study the low-temperature chemistry of interstellar clouds and of extraterrestrial objects in our solar system, such as ice-covered moons and trans-Neptunian objects. See Boogert et al. or Gudipati and Castillo-Rogez for examples [3,4]. To date, astronomical observations from ground- and space-based observatories have provided IR evidence for about a dozen extraterrestrial molecules and ions in the solid phase. Although our title molecule is not among that dozen, laboratory studies of the physical properties and chemical reactions of many yet-undetected species are invaluable for understanding how molecules in extraterrestrial environments can form and evolve.

Of the organic molecules identified in ices by astronomers, methanol (CH_3OH) has received the most detailed and widespread attention, whereas solid ethanol (C_2H_5OH) has almost been ignored by laboratory astrochemists. The recent work of Oba et al. [5] is an exception, making extensive use of earlier IR studies [6,7]. In general, however, a lack of information on amorphous C_2H_5OH, the form expected in many extraterrestrial environments, hinders an understanding, evaluation, and possible observation of ethanol-ice by infrared astronomers. We address this situation in the present paper, beginning with a brief presentation of our earlier far-IR results on amorphous and crystalline ethanol, followed by much newer mid-IR studies. Spectra are presented, apparently for the first time, of amorphous and crystalline ethanol made in a single experiment within the same vacuum chamber. We include values of band strengths for three IR features, a refractive index for amorphous ethanol, a density estimate, and details on phase changes. Our goal is not new detailed spectral analyses and band assignments, but rather the information that IR data can provide on amorphous C_2H_5OH.

2. Experimental

Nearly all of our laboratory procedures and equipment have been described in earlier papers, so a detailed presentation will not be given [8]. Our far-IR spectra were recorded with 4-cm^{-1} resolution on a Mattson Polaris FTIR spectrometer in 1992 using a polyethylene substrate [1]. Our mid-IR spectra were measured recently with a new Thermo iS50 FTIR instrument and a KBr substrate, using 100 scans per spectrum and a resolution of 0.5 cm^{-1}. The high-vacuum chambers (base pressure ~ 10^{-8}) and deposition systems were similar for the two sets of measurements, except that the smaller vacuum chamber had a volume of about 100 cm^3, whereas the larger chamber has a volume of ~300 cm^3. Deposition rates typically gave an increase in the ice's thickness of 1–2 μm h^{-1}. In all cases, the IR beam was unpolarized and perpendicular to the plane of the ice sample. Changes in sample

E-mail address: reggie.hudson@nasa.gov.

http://dx.doi.org/10.1016/j.saa.2017.06.027
1386-1425/Published by Elsevier B.V.

temperature, both warming and cooling, were conducted with the vacuum chamber open to the interfaced, dedicated turbo-molecular pumps. Ethanol (undenatured absolute) and methanol were purchased from Pharmaco and Sigma Aldrich, respectively, and used as received, aside from degassing with freeze-pump-thaw cycles using liquid nitrogen.

3. Results

Fig. 1 shows far-IR spectra of solid ethanol formed by vapor-phase deposition onto a polyethylene substrate held at 13 K. The spectra are somewhat noisy, but the rounded appearance of the peaks in (a) suggests that the initially formed ethanol-ice was amorphous, as is the case with nearly all organic compounds we have studied under similar conditions. As the ethanol sample was warmed, subtle changes were seen in its spectrum, probably reflecting the solid-phase alterations reported by others [9,10]. However, by 115–120 K, considerable sharpening of all spectral bands was observed, indicating the sample's crystallization. These changes are readily seen by comparing traces (a) and (b) in Fig. 1. Few additional changes were met on further warming to 150–155 K, but at 160 K the IR bands of crystalline ethanol returned to their original rounded shapes, shown in trace (c) and suggesting a loss of crystallinity. Recooling to 13 K gave little further change, but rewarming to 120 K again gave the far-IR spectrum shown in (b) and further warming to ~160 K once more gave a spectrum resembling (c). In other words, a temperature sequence along the lines of (a) → (b) → (c) → (a) from Fig. 1 was followed with the IR spectra showing a gain and loss of crystallinity by the sample in each cycle.

These far-IR changes are consistent with recent mid-IR measurements from our laboratory, as presented in Fig. 2. Again, the initially amorphous ethanol sample of spectrum (a) crystallized on warming to give spectrum (b), and again the spectrum reverted to one resembling that of amorphous ethanol on additional warming, and again the temperature sequence (a) → (b) → (c) → (a) could be followed with the same repetition of spectral changes, subject to one condition described below. The temperatures of (b) and (c) in Fig. 2 were chosen to emphasize the small range over which the (b)-to-(c) conversion took place. Differences between (a) and (c) exist in the 3600–3000 cm^{-1} region, but otherwise the similarities between (a) and (c) are quite pronounced, as shown in the expansion of Fig. 3.

Table 1 lists peak positions of some of the more distinct IR features in our spectra of amorphous and crystalline ethanol. These positions agree with expectations from the literature [11–15], but there are disagreements among previous workers on some of the assignments, mainly

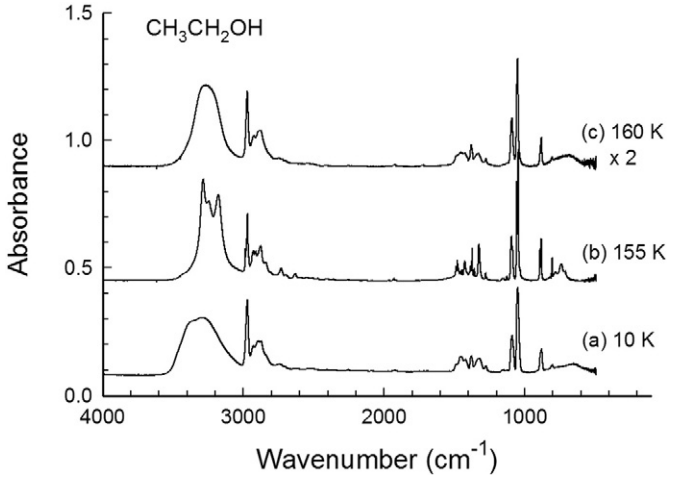

Fig. 2. Mid-IR spectra of ethanol deposited at 10 K and warmed to 155 and 160 K. The sample's original thickness was about 1.5 μm. Spectra have been offset vertically for clarity. Note that the scale of (c) has been expanded by a factor of two to show detail.

those between 1500 and 1300 cm^{-1} and below 400 cm^{-1}, and there is considerable mixing among some of the motions. Some of the identifications are straightforward, such as the broad band near 3200 cm^{-1} being from OH vibrations, the features at 3000–2800 cm^{-1} being from symmetric and asymmetric stretches of CH_3 and CH_2 groups, and the peak near 1050 cm^{-1} being from a C—O stretch.

Repeated tests with ethanol ices between about 0.5 and 8.0 μm in thickness confirmed that above ~155 K a competition existed between a sample's loss of crystallinity and its loss to our vacuum system. Our thicker ices could be put through the temperature sequence of (a) → (b) → (c) → (a) in Figs. 1–3 multiple times with only small variations in IR intensities, from loss to the vacuum, in each cycle. In contrast, our thinner samples were lost before the (b) → (c) conversion occurred. Burke et al. [11] used temperature-programmed desorption to show that for even thinner ethanol ices the first change, (a) → (b), shows a similar thickness dependence, with no crystallization detected for sufficiently thin samples. In all cases, when our ices were left standing at 160 K they were completely lost in few minutes or less depending on the sample's thickness.

Several observations were made on cooling ethanol samples from 160 K to 10, 80, and 100 K. Recooling the sample of (c) in Fig. 2 to either 10 or 80 K at about 6 K min^{-1} preserved the spectrum's general

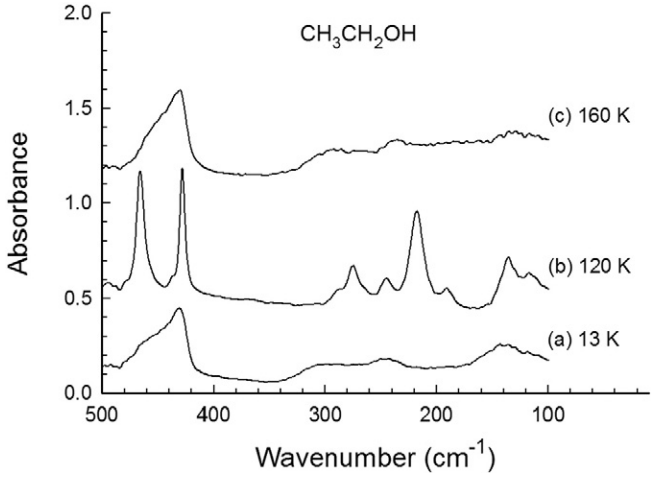

Fig. 1. Far-IR spectra of ethanol deposited at 13 K and warmed to 120 and 160 K. Spectra have been offset vertically for clarity, but not rescaled. The ethanol sample's thickness was not measured accurately at the time, but was ~10 μm.

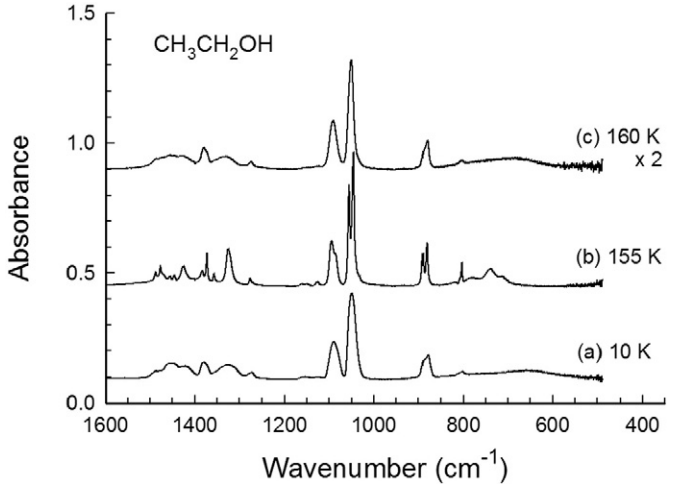

Fig. 3. Expansion of Fig. 2 highlighting the 1600–500 cm^{-1} region. Note the similarity of (a) and (c).

Table 1
Positions (cm^{-1}) of selected IR features of ethanol.

$\nu\sim$ (amorphous, 10 K)	$\nu\sim$ (crystalline, 155 K)
3377, 3298 (broad)	3285, 3247, 3177
2972	2986, 2977, 2970
2930	2928
2897	2911
2874	2879
1487	1488
1478	1477
1457	1461, 1455
1448	1446
1423	1426
1380	1383, 1373
	1357
1326	1325
1275	1278
1090	1094
1050	1055, 1045
886, 879	890, 881
804	803
	741
657 (broad)	
460, 431	466, 428
300	
	275
246	245
	218
	191
139	136
	117

appearance. No spectral changes were seen on allowing such ices to stand overnight at either 10 or 80 K, but rewarming them to ~120 K always regenerated the spectrum of crystalline ethanol in (b) of Fig. 2. Conversely, when the sample of (c) at 160 K was cooled to only 110 K and held there, it inevitably recrystallized in a few hours or less.

The only other changes we wish to document concern the broad 3600–3000 cm^{-1} band of amorphous ethanol. Fig. 4 shows how this feature changed on warming. Ongoing from 10 to 25 K, there was a slight sharpening and a shift in the peak's position, which ended by about 75 K. Subtle additional changes in the peak's shape and position were observed on warming from 100 to 112 K. After about an hour at

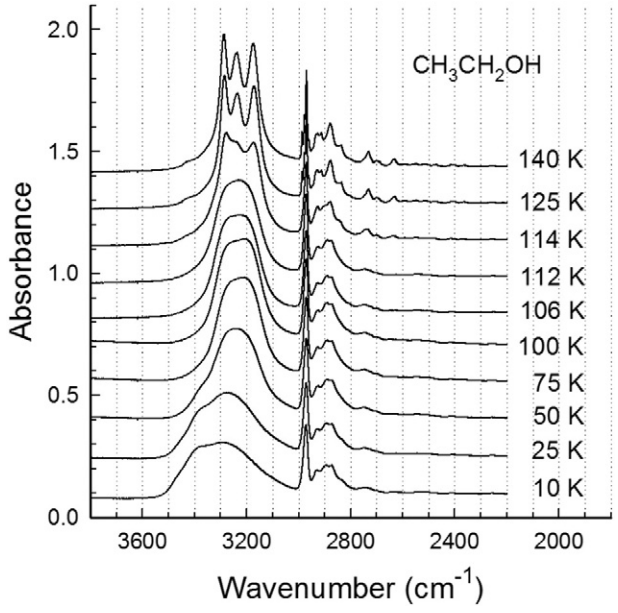

Fig. 4. Ten IR spectra showing changes in the OH and CH stretching regions on warming amorphous ethanol from 10 K to the temperatures indicated. The sample's original thickness was about 1.5 μm. The dotted vertical lines are to assist in judging changes in spectral band shapes and positions. Spectra have been offset vertically for clarity.

114 K evidence of crystallization, the sharp features, appeared, and further warming gave fully crystalline ethanol. None of these changes could be reversed by cooling the crystalline sample, and no such changes were seen with other IR features below 120 K. The only way to reverse the trends in Fig. 4 was to warm the sample to 160 K and then to quickly cool it, with the results already described. Even then, spectrum (a) in our Fig. 4 was never recovered, but rather the spectrum after annealing most resembled those at 100 or 106 K in the middle of the same figure.

Related to all of our experiments was the need to quantify the thickness of each sample. We addressed this problem by measuring the refractive index of amorphous ethanol and using standard relations to calculate an ice thickness from interference fringes [8]. Multiple measurements at 16 K by two-laser interferometry gave $n(670\ nm) = 1.26 \pm 0.01$. Support for this value comes from an independent measurement by Dobryshev et al. [16] that gave $n(633\ nm) = 1.25 \pm 0.02$ at 16 K with the same technique we used.

Ice thicknesses also can be determined by using absolute band intensities (A) and absorption coefficients (α) derived from optical constants, but these have not been published for amorphous ethanol. As an alternative, we measured apparent absorption coefficients (α') and apparent band strengths (A') of three ethanol features having minimal overlap with other absorbances. First, ethanol's room-temperature refractive index (n) of 1.3611 and density (ρ) of 0.7893 g cm^{-3} [17] were used with the Lorentz-Lorenz Eq. (1)

$$\rho = \left(\frac{1}{r}\right)\left(\frac{n^2-1}{n^2+2}\right) \quad (1)$$

to give a specific refraction (r) of 0.2804 $cm^3\ g^{-1}$, so that our own $n = 1.26$ implies a density of 0.584 g cm^{-3}. This density and the usual Beer's Law plots (correlation coefficients > 0.99) in turn gave the α' and A' values summarized in Table 2 for amorphous ethanol. More-accurate values will require a better determination of ethanol's density near 10 K, or perhaps a measurement of amorphous ethanol's polarizability near that temperature, from which a better specific refraction can be found.

It is difficult to compare the ethanol band strengths of Table 2 with those of other amorphous alcohols as, to our knowledge, none have been measured directly. The safest comparison seemed to be to record spectra of amorphous CH_3OH (methanol) under the same conditions we used for amorphous CH_3CH_2OH (ethanol). Accordingly, three ices with roughly the same thickness (1.5 μm) were grown at 16 K for each compound, their IR spectra recorded, and the bands in the 3000–2800 cm^{-1} region, for CH stretches, integrated. The CH_3OH samples had a greater integrated absorbance, but with a lower molecular weight for CH_3OH compared to CH_3CH_2OH, the methanol samples also had a greater column density of molecules. This resulted in the two compounds having about the same apparent band strength, $A' \sim 2 \times 10^{-17}$ cm $molecule^{-1}$, in this region given the uncertainties in the supporting data (n and ρ) for methanol. We plan to return to this comparison after a more-complete treatment of n and ρ for CH_3OH is available.

4. Discussion

The IR changes of Figs. 1–3 suggest that warming amorphous ethanol from ~10 to 160 K under vacuum carried the ice through an amorphous-crystalline-amorphous sequence involving two solid-solid phase transitions. However, solid ethanol has been studied for almost a century by calorimetric methods, which have established a freezing point of 159 K for the compound [18]. Therefore, the correct interpretation of our results is simply that the first transition observed, near 120 K, is a crystallization, and that as the crystalline sample then was warmed past 159 K it converted into liquid ethanol with a low vapor pressure at that temperature. When subsequently cooled, the liquid produced an

Table 2
Intensities of three infrared features of amorphous ethanol at 10 K.

$\nu\sim$ (cm^{-1})	α' (cm^{-1})[a]	Integration range (cm^{-1})	A' (10^{-18} cm molecule^{-1})[b]	Approximate description[c]
1090	2746	1113–1067	7.35	CCO asymmetric stretch
1050	6340	1067–1011	14.10	CO stretch
886, 879	1328	920–860	3.24	CCO symmetric stretch

[a] From the slopes of Beer's Law graphs of 2.303 × (peak height) against ice thickness. In each case, the slope is the apparent absorption coefficient, α'.
[b] From the slopes of Beer's Law graphs of 2.303 × (band area) against ice thickness. In each case, the slope divided by (ρN_A/MW) gives A', where MW = molecular weight = 46.07 g mol^{-1}, $N_A = 6.022 \times 10^{23}$ molecules mol^{-1}, and density = 0.584 g cm^{-3}. For recent examples see reference [8].
[c] Assignments from [11–15], and references therein.

amorphous solid or perhaps a supercooled liquid, which could be recrystallized on again warming to ~120 K. Our assignment of traces (c) in Figs. 1–3 to liquid ethanol is also supported by a spectrum of the liquid recorded at room temperature, the spectrum being calculated from optical constants [19,20]. See Fig. 5 for the comparison. The similarity of the three spectra is particularly striking when one considers the wide range of temperatures used to record them.

Ethanol at low pressures has an unusually rich set of condensed phases, and it is interesting to compare our work to what is known about them [9,10,16,21–23]. With ethanol's phase diagram in mind, the changes in Fig. 4 for amorphous ethanol's broad 3300-cm^{-1} feature on warming correspond roughly to the formation of a second amorphous (glassy) solid on warming to ~75 K, and then a change to a supercooled liquid at 97 K, ethanol's glass transition temperature [18]. The small spectral changes on continued warming past ~110 K can be attributed to a conversion of the supercooled liquid into a plastically crystalline phase, and then finally a monoclinic crystalline phase above about 115 K. Following liquefaction at 160 K, samples then were cooled at about 6 K min^{-1}, slow enough to suggest that either a supercooled liquid or the plastic crystalline modification of ethanol were the first formed, which then converted to the monoclinic phase on sitting at 115 K. However, liquid ethanol samples that were cooled and held below 97 K, ethanol's glass transition temperature [18], failed to recrystallize until the temperature was again raised to 115–120 K, just as expected for a glass cooled from a melt [24]. The fact that most of the changes seen on warming from 10 to ~115 K were restricted to the broad feature around 3300 cm^{-1} suggests that considerable rearrangement of the H-bonding network in solid ethanol was occurring. Clearly some of the spectral changes in Fig. 4 are quite subtle, and more work is needed to explore connections to ethanol's phase diagram.

Concerning other results, our band strengths and refractive index n(670 nm) can be used to measure the vapor pressure and enthalpy of sublimation (ΔH_{subl}) of solid ethanol [25]. Also, by forming appropriate ratios with our A' and α' values, apparent band strengths and absorption coefficients can be estimated for features in the spectra of solid ethanol other than those in Table 2, including features in the crystalline phase and in the near- and far-IR regions. The asymmetric shape of the 883 and 480–420 cm^{-1} spectral features almost certainly derives from two ethanol conformational isomers, the *trans* (*anti*) and *gauche* (the lesser stable) conformers [12,13], but to our knowledge these have not been studied in neat amorphous ethanol.

Our results also have connections to recent work on an isovalence-electronic molecule, ethanethiol, by Pavithraa et al. [26]. Those authors reported changes in the mid-IR spectra of CH_3CH_2SH strongly resembling what we have presented here for CH_3CH_2OH. Their amorphous ethanethiol samples crystallized on warming to about 120 K, but additional heating to 125–130 K produced IR spectra resembling those of the original amorphous solid. The authors also found that the changes observed depended on the thickness of their CH_3CH_2SH ices in a manner similar to what we have found for CH_3CH_2OH. We do not believe that such changes should be considered as, in those authors' words, a "remarkable transformation from crystalline phase to amorphous phase at higher temperatures". Given that ethanethiol converts from a solid to a liquid phase at 125 K [27], a more mundane explanation is applicable - melting.

5. Conclusions

The original motivation for this paper came from the possible use of our data by astronomers and astrochemists. However, our spectra show that most, but not all, of the IR features for CH_3CH_2OH, and also CH_3CH_2SH, overlap with the IR bands of frozen H_2O or interstellar silicate grains. Our results also show that methanol and ethanol have similar intrinsic band strengths in the regions used for CH_3OH detection by astronomers. Moreover, given the complexity of CH_3CH_2OH and CH_3CH_2SH compared to CH_3OH and CH_3SH, there is an expectation that the former pair will be the one of lower abundance. These factors conspire to make the prospect of a remote-sensing detection of frozen CH_3CH_2OH and CH_3CH_2SH rather dim. Nevertheless, the present work contains useful results on the temperature ranges for ethanol's solid phases, the compound's refractive index, the estimate of a density, and our A' and α' measurements. This information can be applied, for example, in a selection of starting conditions for an IR determination of branching ratios for ethanol ice's destruction by ionizing radiation. Needed for such experiments are a choice of temperature, a measurement of the size of the ice sample, and the selection of spectral bands to monitor, all covered by our work. Similar comments apply to photodestruction experiments on ethanol ice to determine lifetimes in various extraterrestrial environments and also to reactions designed to produce ethanol under interstellar conditions.

The ethanol work presented here, and that published for ethanethiol [26], show that it is possible to warm an amorphous organic-molecular solid under high vacuum to where it converts into a liquid, and then to record its IR spectrum before evaporation. Such a "liquefaction-before-

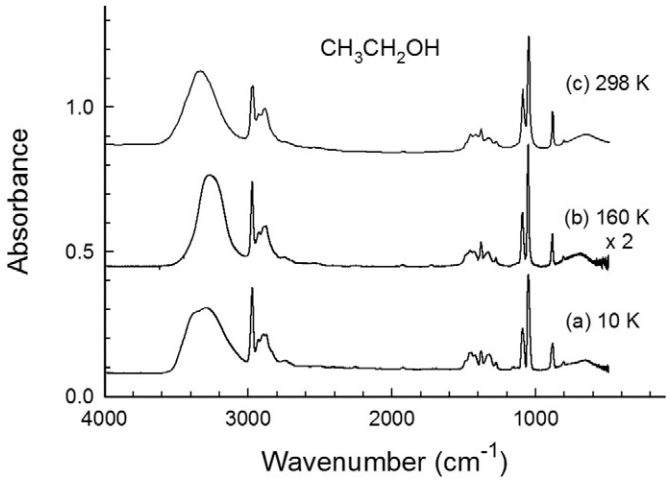

Fig. 5. A comparison of the IR spectra of (a) amorphous solid ethanol at 10 K and (b) the same sample warmed to 160 K with (c) a spectrum of liquid ethanol at room temperature. See Section 4 of the text for details. Spectra have been offset vertically for clarity.

sublimation" is less likely to be seen the lower a vacuum system's base pressure and the higher the ice sample's melting point. If a severe, but temporary, degradation of one's vacuum conditions can be tolerated then such a transformation might permit comparisons of, for example, vapor pressures and enthalpies of sublimation and vaporization of solid and liquid ethanol within the same vacuum chamber and at similar temperatures. Lastly, although CH_3CH_2OH and CH_3CH_2SH are the first two organic compounds we have encountered that show liquefaction under the stated conditions, we predict that others of similar size and complexity await discovery.

Acknowledgment

The far-IR work for this project was undertaken in 1992 while RLH was on a leave-of-absence from a faculty position at Eckerd College (Florida, USA). The support of that institution's faculty, staff, administration, and trustees is gratefully acknowledged. Our recent mid-IR ethanol measurements were supported by funding from NASA's Astrophysics Research and Analysis (APRA) program. NASA co-workers Perry Gerakines and Mark Loeffer are acknowledged for helpful conversations, and Andrey Drobyshev (Al-Faraibi Kazakh National University, Kazakhstan) is thanked for reprints and preprints.

References

[1] M.H. Moore, R.L. Hudson, Far-infrared spectra of cosmic-type pure and mixed ices, Astron. & Astrophys. Suppl. Ser. 103 (1994) 45.
[2] B.A. McGuire, S. Ioppolo, M.A. Allodi, G.A. Blake, THz time-domain spectroscopy of mixed CO_2-CH_3OH interstellar ice analogs, Phys. Chem. Chem. Phys. 18 (2016) 20199.
[3] A.C.A. Boogert, P.A. Gerakines, D.C.B. Whittet, Observations of the icy universe, Annu. Rev. Astron. Astrophys. 53 (2015) 541.
[4] M. Gudipati, J. Castillo-Rogez (Eds.), The Science of Solar System Ices, Springer, New York, 2013.
[5] Y. Oba, K. Osaka, T. Chigai, A. Kouchi, N. Watanabe, Hydrogen-deuterium substitution in solid ethanol by surface reactions at low temperatures, Mon. Not. Royal Astro. Soc. 462 (2016) 689.
[6] J. Perchard, M. Josien, Vibrational spectra of twelve isotopic monomeric ethanol species, J. Chim. Phys. 65 (1968) 1834.
[7] J. Perchard, M. Josien, Study of the vibrational spectra of twelve isotopic species of autoassociated ethanols, J. Chim. Phys. 65 (1968) 1856.
[8] R.L. Hudson, Infrared spectra and band strengths of CH_3SH, an interstellar molecule, Phys. Chem. Chem. Phys. 18 (2016) 25756.
[9] A. Drobyshev, A. Aldiyarov, K. Katpaeva, E. Korshikov, V. Kurnosov, D. Sokolov, Transformation of cryovacuum condensates of ethanol near the glass transition temperature, Low Temp. Phys. 39 (2013) 919.
[10] M.A. Ramos, M. Hassaine, B. Kabtoul, R.J. Jimenez-Riobóo, I.M. Shmyt'ko, A.I. Krivchikov, I.V. Sharapova, O.A. Korolyuk, Low-temperature properties of monoalcohol glasses and crystals, Low Temp. Phys. 39 (2013) 468.
[11] D.J. Burke, A.J. Wolff, J.L. Edridge, W.A. Brown, The adsorption and desorption of ethanol ices from a model grain surface, J. Chem. Phys. 128 (2008) 104702.
[12] A.J. Barnes, H.E. Hallam, Infrared cryogenic studies. Part 5. Ethanol and ethanol-d in argon matrices, Trans. Faraday Soc. 66 (1970) 1932.
[13] S. Coussan, Y. Bouteiller, J.P. Perchard, W.Q. Zheng, Rotational isomerism of ethanol and matrix isolation infrared spectroscopy, J. Phys. Chem. A 102 (1998) 5789.
[14] Y. Mikawa, J.W. Brasch, R.K. Jakobsen, Polarized infrared spectra of single crystals of ethyl alcohol, Spectrochim. Acta 27A (1971) 529.
[15] J.R. Durig, C.W. Hawley, Low-frequency modes in molecular crystals. 17. Torsional motions and barriers to internal rotation in some ethylsilanes, ethylgermanes, and ethanol, J. Phys. Chem. 75 (1971) 3993.
[16] A. Drobyshev, A. Aldiyarov, D. Sokolov, A. Shinbayeva, N. Tokmoldin, Refractive indices of cryovacuum deposited thin films of ethanol, methane, and nitrous oxide in the vicinity of their phase transition temperatures, Low Temp. Phys. (2017) (in press).
[17] R. Weast (Ed.), CRC Handbook of Chemistry and Physics, 61st EditionCRC Press, Boca Raton, Florida, 1980.
[18] K.K. Kelley, The heat capacities of ethyl and hexyl alcohols from 16 K to 298 K. And the corresponding entropies and free energies, J. Amer. Chem. Soc. 51 (1929) 779.
[19] E. Sani, A. Dell'Oro, Spectral optical constants of ethanol and isopropanol from ultraviolet to far infrared, Opt. Mater. 60 (2016) 137.
[20] R. Swanepoel, Determination of the thickness and optical constants of amorphous-silicon, J. Phys. E. - Sci. Instr. 16 (1983) 1214.
[21] O. Haida, H. Suga, S. Seki, Calorimetric study of the glassy state XII. Plural glass-transition phenomena of ethanol, J. Chem. Therm. 9 (1977) 1133.
[22] M.A. Ramos, I.M. Shmyt'ko, E.A. Arnautova, R.J. Jiménez-Riobóo, V. Rodrıguez-Mora, S. Vieira, M.J. Capitán, On the phase diagram of polymorphic ethanol: thermodynamic and structural studies, J. Non-Cryst. Solids 352 (2006) 4769.
[23] A. Drobyshev, E. Korshikov, V. Kurnosov, D. Sokolov, On the problem of the existence of a supercooled liquid phase of cryovacuum ethanol condensates, Phys. Solid State 54 (2012) 1475.
[24] I.S. Gutzow, J.W.P. Schmelzer, The Vitreous State, 2nd edition Springer, New York, 2013 28.
[25] R.K. Khanna, J.E. Allen Jr., C.M. Masterton, G. Zhao, Thin-film infrared spectroscopic method for low-temperature vapor pressure measurements, J. Phys. Chem. 94 (1990) 440.
[26] S. Pavithraa, R.R.J. Methikkalam, P. Gorai, J.-I. Lo, A. Das, B.N. Raja Sekhar, T. Pradeep, B.-M. Cheng, N.J. Mason, B. Sivaraman, Qualitative observation of reversible phase change in astrochemical ethanethiol ices using infrared spectroscopy, Spectrochim. Acta 178A (2017) 166.
[27] J.P. McCullough, D.W. Scott, H.L. Finke, M.E. Gross, D. Williamson, R.E. Pennington, G. Waddington, H.M. Huffman, Ethanethiol (ethyl mercaptan): thermodynamic properties in the solid, liquid, and vapor states. Thermodynamic functions to 1000 K, J. Amer. Chem. Soc. 74 (1952) 2801.